A computer vision-based fast approach to drilling tool condition monitoring

A Volkan Atli[1], O Urhan[1,2], S Erturk[1,2]*, and **M Sonmez[1]**
[1]Electronics and Telecommunications Engineering Department, University of Kocaeli, Kocaeli, Turkey
[2]LATARUM Research Centre, University of Kocaeli, Kocaeli, Turkey

The manuscript was received on 16 June 2005 and was accepted after revision for publication on 15 May 2006.

DOI: 10.1243/09544054JEM412

Abstract: A computer vision-based approach to drilling tool condition monitoring is proposed in this paper. Firstly, image frames are captured using a high-speed CCD camera. Then, a canny edge detector is employed to extract tool features from the acquired images. In order to obtain a measure of tool wear, the deviation from linearity (DEFROL) metric is proposed. Experimental results show that the proposed method detects the condition of all tested tools successfully.

Keywords:

1 INTRODUCTION

Tool condition monitoring is used in modern manufacturing environments to reduce machine tool downtime and facilitate optimum utilization of unsupervised machining centres. Particularly with recent advances and applications in high-speed machining, there is an increasing demand for high precision and accuracy, while the most serious problem in high-speed machining is regarded as being increased product cost and reduced product quality as a result of severe tool wear [**1**]. Tool condition monitoring is required particularly to detect tool wear and avoid tool breakage to protect the product as well as machinery.

Tool wear has long been identified as the most undesirable characteristic of machining operations. Tool wear is caused by the physical and chemical interactions between the cutting tool and workpiece, and can be described as the removal of small parts from the material at the cutting edge of the tool as a result of these interactions.

Tool wear measurement methods can be divided mainly into two classes: direct and indirect measuring methods [**2**]. In direct measuring, the cutting edge of the tool is monitored using a machine vision system, an optical microscope, or a tactile sensor, for instance. Indirect measuring methods measure the degree of tool wear using sensors that generate signals that indirectly provide information about the tool condition, such as force, vibration, or acoustic emission sensors [**3–6**].

In [**2**], a tool wear measuring system using a CCD camera and an exclusive jig was constructed to reduce the time delay caused by the tool detachment process in optical microscope systems. It has been noted in [**7**] that advances in machine vision and image processing technology have led to the development of various in-cycle vision sensors used to obtain information about the cutting tool and machined part. As long as the tool is not in permanent contact with the machined part, on-line monitoring can be achieved with vision systems without the need for any physical contact. The authors of [**7**] go so far as to argue that the potential of vision-based tool condition monitoring techniques is unlimited. As a broad review is provided in the corresponding paper the same techniques will not be paraphrased in this paper and the reader is referred to [**7**] for this purpose. It is, however, useful to state that the typical sequence for determining cutting tool flank wear parameters using a machine vision system are stated in [**7**] to be: image enhancement, image segmentation, breakage detection, and tool wear parameter derivation. In [**8**], machine vision is used to assess surface roughness of machined parts produced by shaping and milling processes, where quantitative measures of surface roughness, that

**Corresponding author: Electronics and Telecommunications, Engineering Department, University of Kocaeli, Kocaeli, Turkey. email: sarp@ieee.org*

are extracted in the spatial frequency domain using a two-dimensional Fourier transform, are forwarded to two artificial neural networks, which take roughness features as input and determine the surface roughness. A tool condition monitoring system that combines sound and image analysis is proposed in [**9**], where two separate texture analysis approaches referred to as column projection and run-length statistical methods are presented to analyse machined surfaces. In [**10**], the performance of three image-processing algorithms, in estimating the tool condition, is presented: analysis of the intensity histogram; image frequency domain content; and spatial domain surface texture. Fractal analysis of surface texture for tool wear monitoring is proposed to deal with high directionality and self-affinity of machined surfaces and a hidden Markov model is used to differentiate the states of tool wear in [**11**]. Statistical filtering of images of the cutting edge for worn area detection is utilized to decide tool condition in [**12**]. In [**13**], surface images are first preprocessed by a Canny edge detector, and then applied to a connectivity-oriented fast Hough transform to detect all the line segments, after which the distributions of the orientations and lengths of the line segments are used to determine tool wear. In [**14**], a laser diode is used to project a line stripe onto a surface and obtain three-dimensional information from the straightness of the line pattern. The utilization of a mathematical tool model and geometry for flank wear detection; and image consolidation and dilation for crater wear detection using a neural network is presented in [**15**]. In [**16**], a possible classification of defects in cutting inserts and the design of an automated sensor to recognize defects and measure tool wear is presented. A laser displacement meter is used to obtain the three-dimensional laser image of milling cutters and image analysis for the recognition and measurement of ball end mill inspection is presented in [**17**]. In [**18**], a system that captures and processes successive moving images of inserts to measure flank wear in milling by making use of the relationship between successive image pairs is presented. A review of state-of-the-art methods and results in tool condition monitoring is provided in [**19**].

This paper proposes a new and, most importantly, fast tool condition monitoring approach using a computer vision system. A genuine tool condition measure referred to as deviation from linearity (DEFROL) is developed to monitor drilling tool flank wear. A simple segmentation approach that is optimized for the machining system so as to eliminate the need for preceding image enhancement, followed by the genuine DEFROL measure enables fast and reliable tool condition monitoring.

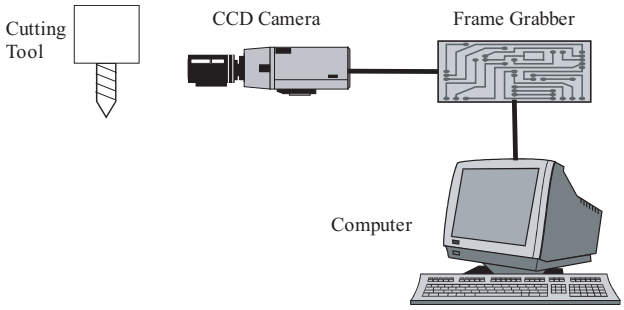

Fig. 1 Computer vision-based tool wear monitoring system

2 THE COMPUTER VISION-BASED MONITORING SYSTEM

Figure 1 displays the computer vision-based tool wear monitoring system utilized in the approach presented in this paper. Cutting tool tests are conducted on a computer numerical controlled (CNC) four-axis machining centre. For the drilling process, holes are drilled on a cast-iron workpiece material using HSS drill bits with various diameters. The holes were drilled typically to a depth of 20 mm. Different feed rates (300 and 450 mm/min) in drilling and spindle speeds (1600 and 1800 r/min) were used to obtain different tool wear rates. In addition to this, the cutting conditions (spindle speed, feedrate, and depth of hole) remained constant throughout the tests. All tests were performed without using any cutting fluid, i.e. under dry cutting conditions. The workpiece materials were fairly homogeneous and their geometrical features were not considered. A Roper Scientific ES310T high-speed CCD camera is used to acquire the images. The camera has a pixel resolution of 648×484 pixels, is capable of acquiring 125 frames/s, and is equipped with a 12 mm F1.2 lens. The camera is located at a distance of about 15 cm to the tool and focused so that it sharply captures the cutting tool, but the background is blurred. A National Instruments NI 1424 PCI frame grabber is used to read the images into the computer. A light source is located about the camera location pointing towards the cutting tool, to provide sufficient illumination.

In order to assess tool condition, images are captured after the drill tool is raised above the workpiece. Hence, effects such as chip formation will not be observed in the captured image. Figure 2 shows sample images from an undamaged tool captured with the utilized monitoring system. The images are actually of size 400×400 pixels and therefore have higher resolution and more sharpness, but are displayed here in down-sampled form. Figures 3 and 4 show example images of worn tools.

Fig. 2 Sample images of a sharp drilling tool

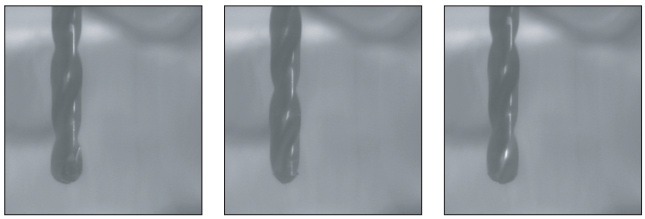

Fig. 3 Sample images of a worn drilling tool

Fig. 4 Sample images of another worn drilling tool

It is important to note that the background is blurred, while the tool has more sharpness as the camera is focused according to tool location. Hence, it becomes possible to extract tool features with no need for preceding image enhancement. Because the tool has more sharpness, the tool silhouette can successfully be extracted using edge detection techniques, while any background contribution is avoided during this process. As seen in Figs 2–4, the acquired background might change according to tool head location, but as the background is blurred, it has no effect on the process of detecting the tool tip.

3 THE DEVIATION FROM LINEARITY (DEFROL) MEASURE

In order to extract tool features from the acquired images, Canny edge detection is utilized [**20**]. This technique provides a sophisticated approach to detect the edges encountered in an image. While there is basically a trade-off between noise reduction and edge localization, canny edge detection provides the best possible compromise between these requirements, and although the Canny detector is optimized for step edges in the presence of Gaussian noise, it is observed to provide good results for real images.

In order to suppress image noise, the first step of Canny edge detection consists of image smoothing, using a Gaussian low-pass filter. The two-dimensional Gaussian filter function is defined as

$$h(x,y) = \exp\left[\frac{-(x^2+y^2)}{2\sigma^2}\right] \tag{1}$$

where the standard deviation σ determines the width of the filter and, hence, the amount of smoothing. A larger standard deviation will provide more noise suppression; however, weak edges will also be smoothed away. In practice, it is possible to preconstruct a fixed size two-dimensional filter kernel with elements corresponding to the Gaussian filter values, and filtering can be carried out through the convolution of the image with this filter kernel.

In order to enhance edges, horizontal and vertical gradients are computed in the form of

$$\begin{aligned} g_x(x,y) &= I(x+1,y) - I(x-1,y) \\ g_y(x,y) &= I(x,y+1) - I(x,y-1) \end{aligned} \tag{2}$$

and the gradient magnitude and direction are computed using

$$\begin{aligned} g &= \sqrt{g_x^2 + g_y^2} \\ \theta &= \arctan\left(\frac{g_y}{g_x}\right) \end{aligned} \tag{3}$$

where g is used to denote the magnitude and θ is used to denote the direction of the gradient at any pixel location. Image-smoothing and edge enhancement can be combined for a fast implementation by convolving the image with a derivative of Gaussian kernel. It becomes possible further to exploit separability and carry out the computation with one-dimensional kernels to speed up the process.

The edge localization stage consists of two steps, namely non-maximal suppression and hysteresis thresholding. Non-maximal suppression is the process of thinning wide ridges around local maxima in gradient magnitude obtained using equation (3), until every edge is only one pixel wide. Making use of the gradient magnitudes and directions computed using equation (3), for non-maximal suppression, gradient magnitudes that are smaller than gradient magnitudes of neighbour pixels in the direction of the gradient are removed from the gradient map. Hysteresis thresholding uses two thresholds, one low threshold th_{low} and one high threshold th_{high}, to overcome the problems associated with standard single and fixed threshold approaches. The high threshold value is used to mark the best edge pixel locations, and edges are constructed starting from

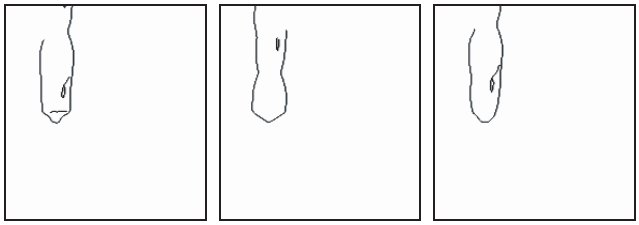

Fig. 5 Sample edge detection results for a sharp drilling tool

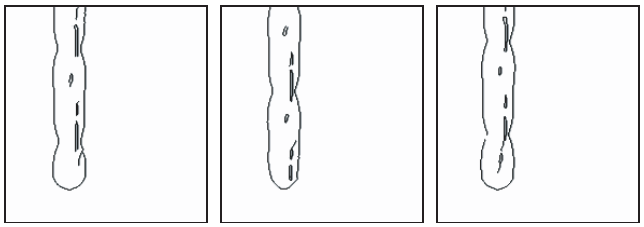

Fig. 6 Sample edge detection results for a worn drilling tool

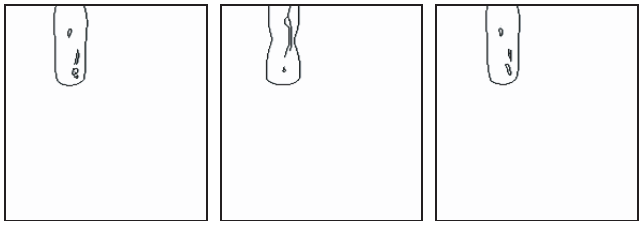

Fig. 7 Sample edge detection results for another worn drilling tool

these locations by searching for neighbours that have a gradient magnitude that is above the low threshold value. To further speed up the process, only neighbour pixels that are along a line normal to the gradient magnitude direction are taken into consideration.

Figures 5, 6, and 7 demonstrate the canny edge detection results for sharp as well as worn tools. Note that the standard deviation of the smoothing filter as well as the low and high threshold values of the hysteresis thresholding are adjusted to extract tool features and disregard the background.

To determine precisely the location of the tool, the image size is reduced by approaching from the bottom, right, and left of the image until the first pixel location is reached. This process is displayed in Fig. 8 and provides accurate and fast localization of the tool.

In order to obtain the accurate location of the tool tip, the slope of the tool outline is computed for two neighbour pixels located on the tool edge, in an upward direction. It is analysed that the tool tip has been enclosed if this slope is sufficiently close to a

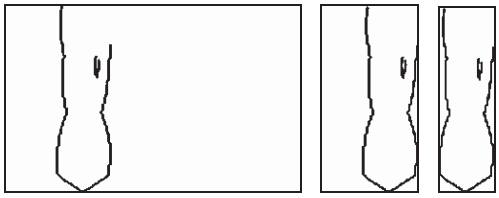

Fig. 8 Localization of the tool

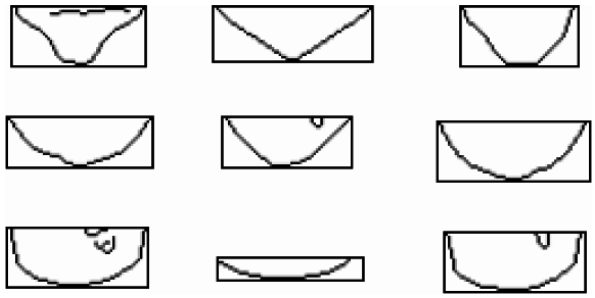

Fig. 9 Example tool tip outlines

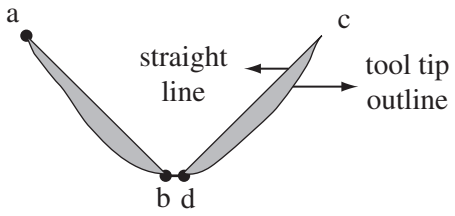

Fig. 10 Computation of DEFROL values

vertical line. Sample results of this process are displayed in Fig. 9.

In order to obtain a measure of drill tool wear, the DEFROL metric is proposed in this paper. For this purpose, the right and left halves of the tool tip are processed separately, as shown in Fig. 10. Two points are selected each on the right and left halves, one near the bottom of the tip and the other near the top. In Fig. 10, 'a' denotes the point at the top of the tip and 'b' denotes the point on the bottom of the tip for the left-hand side of the tool; while 'c' denotes the point at the top of the tip and 'd' denotes the point on the bottom of the tip for the right-hand side of the tool. These points are then connected with straight lines, as displayed in Fig. 10. To measure the DEFROL, the total number of pixels lying between these lines and the tool tip outline are finally counted (i.e. the number of pixels within the grey area shown in Fig. 10). It is expected that this number naturally will be low in the case of a sharp tool when the flanks are viewed directly with the camera, while a higher DEFROL value is obtained for worn tools.

As the cutting tool is rotating, the camera will not always see the flanks directly, so that the DEFROL value might also increase for sharp tools in some

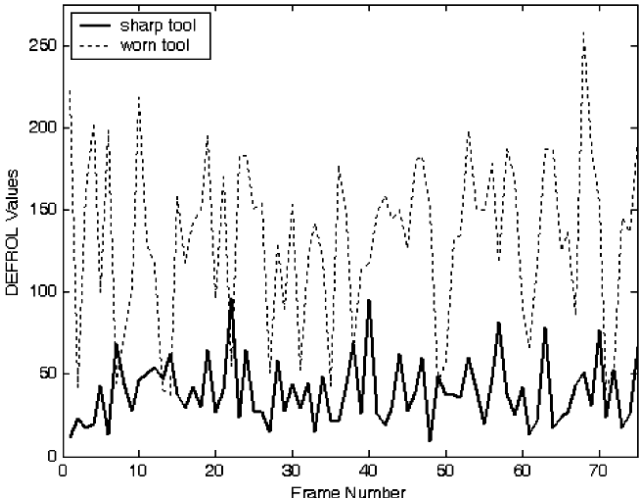

Fig. 11 DEFROL values of a sharp and a worn HSS drill tool with a diameter of 6 mm

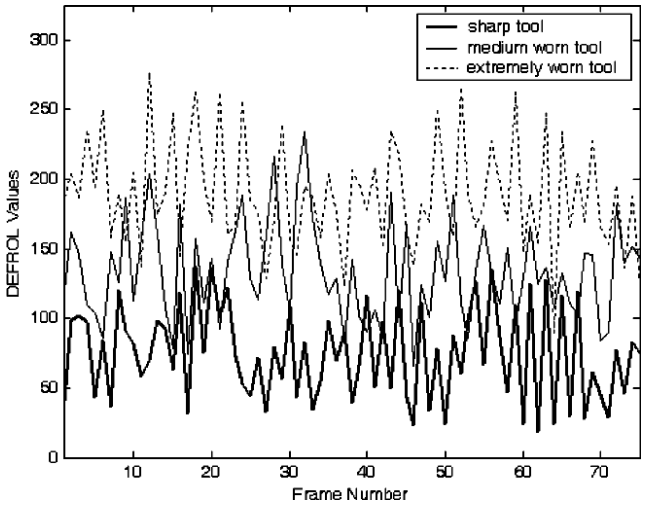

Fig. 12 DEFROL values of a sharp, a medium worn, and an extremely worn HSS drill bit with a diameter of 8 mm

frames. However, if the frame speed is sufficiently high an appropriate view will be captured every few frames, so that the DEFROL value will drop to a comparably lower value every few frames for a sharp tool.

4 EXPERIMENTAL RESULTS

Figure 11 shows the DEFROL values computed for several consecutive frames of a sharp and a worn HSS drill tool with a diameter of 6 mm. It is seen that the DEFROL values of the worn tool are significantly higher than those of the sharp tool. Not only is there a considerable difference in average (i.e. mean) value of the DEFROL measure over time, but also the DEFROL values of the sharp tool drop to extremely low values every few frames, while the DEFROL measure never falls to the same extremely low level for the worn tool. Hence, it becomes easily possible to differentiate between sharp and worn tools using the proposed DEFROL measure.

Figure 12 shows the DEFROL values for a sharp, a medium worn, and an extremely worn HSS drill bit with a diameter of 8 mm. This figure clearly shows that the DEFROL values increase with the amount of wear. For a sharp tool, the DEFROL values are considerably low, while the DEFROL values rise while the drill tool becomes worn and significantly higher values are obtained for an extremely worn tool. Compared to the DEFROL tools for drill bits with 6 mm diameter shown in Fig. 11, it is observed that the DEFROL values are higher for drill bits with 8 mm diameter. This is expected as the tool tip width detected in the image will increase with higher tool diameter, and hence the number of pixels calculated in the DEFROL measure is also expected to increase with tool diameter.

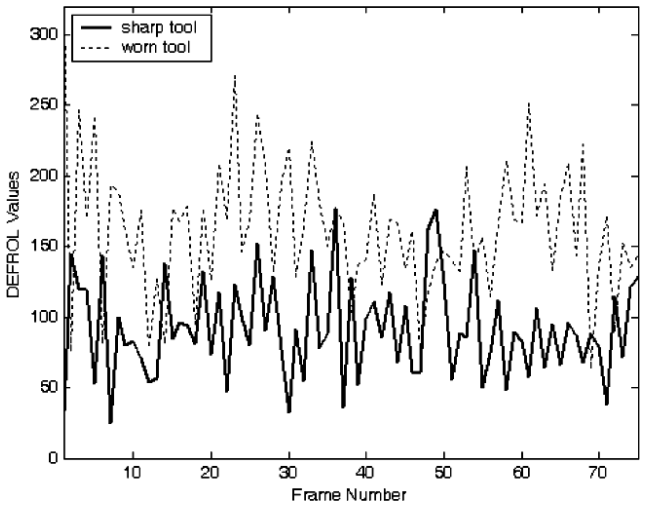

Fig. 13 DEFROL values of a sharp and a worn HSS drill bit with a diameter of 9 mm

Figures 13 and 14 show the DEFROL values for a sharp and worn HSS drill bit with a diameter of 9 mm and 12 mm respectively. It is again seen that the DEFROL measure takes a considerably higher average for worn tools and also the lowest value, to which the DEFROL measure falls, is significantly higher for worn tools compared to sharp tools. It becomes possible, therefore, to differentiate easily between sharp and worn tools and constantly monitor the wear status of a drill tool.

From Figs 11–14 it is seen that the DEFROL measure is actually related to the tool diameter. The average values of the DEFROL measure for sharp and worn tools for different diameters are given in Table 1. Furthermore Fig. 15 shows the average values of the DEFROL measure for sharp tools plotted against tool diameter and it is seen that the

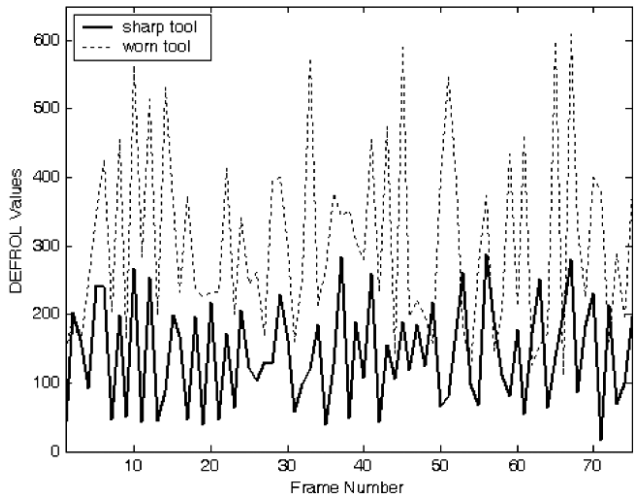

Fig. 14 DEFROL values of a sharp and a worn HSS drill bit with a diameter of 12 mm

Table 1 Average DEFROL value for sharp and worn HSS drill bits with diameters of 6, 8, 9, and 12 mm

	Average DEFROL value according to tool diameter			
Tool diameter	6 mm	8 mm	9 mm	12 mm
Sharp tool av. DEFROL	39.42	74.59	91.59	142.92
Worn tool av. DEFROL	131.93	189.33	162.35	303.05

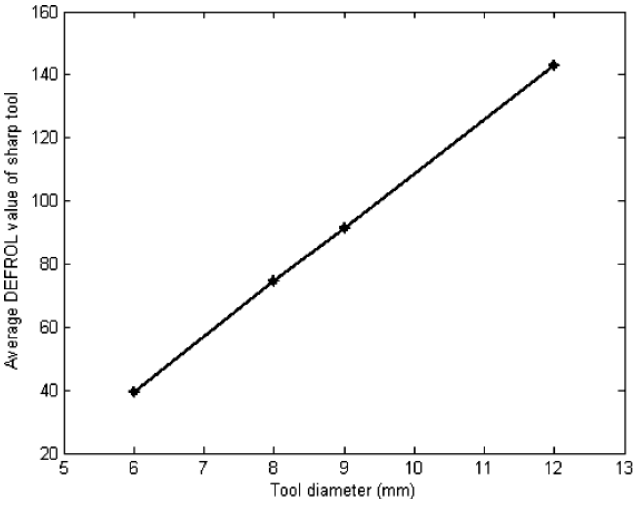

Fig. 15 Average DEFROL values of a sharp HSS drill bit plotted against tool diameter

average value changes fairly linear with respect to tool diameter. It is possible, therefore, to obtain a unique classification by dividing the DEFROL value by the tool diameter if tools of different diameters are to be utilized, with the corresponding tool diameter being entered by the operator.

Figures 11–14 show that the DEFROL value drops to low values for sharp tools every few frames and is on average usually low valued, while it remains considerably higher for worn tools, so that worn tools can be distinguished easily automatically. Experiments show that it is possible to classify sharp or worn tools according to the average of DEFROL measures computed in a certain time window, as the average over several frames will be considerably lower for sharp tools compared to worn tools. Furthermore, it is also possible to perform this classification according to the minimum value of the DEFROL measure within a sliding window (i.e. within a certain frame neighbourhood). The size of the sliding window is related to the camera frame rate and the speed of the tool as the camera should see the flanks at least once within this window. This process has been found to be faster and also more reliable than taking the average.

As seen in Figs 11–14, the DEFROL measure falls to low values (close to zero) for sharp tools. While the tool is worn, the minimum value of the DEFROL measure within the sliding window will steadily increase. It is found that the minimum value of the DEFROL measure increases significantly once the tool is excessively worn and unusable. Hence, it is simple to construct a reasonable threshold value based on experimental observations. Furthermore, as an increase in the minimum DEFROL value is directly a measure of wear intensity, it is possible to track wear intensity using this value instead of only making a sharp/worn decision.

The proposed approach has been tested on 40 HSS drill bits with various diameters of 6, 8, 9 and 12 mm, and all tools have been classified correctly. As seen from Figs 11–14, the proposed DEFROL measure takes significantly different values for sharp and worn tools, hence reliable classification is accomplished.

5 CONCLUSIONS

Tool condition monitoring is an important requirement for many modern manufacturing processes, particularly in drilling and cutting applications. This paper proposes a new and, most importantly, fast drilling tool condition monitoring approach using a computer vision system. A genuine tool condition measure referred to as DEFROL is proposed to monitor drilling tool wear. A simple tool outline segmentation approach that is optimized for the machining system, and the proposed DEFROL measure enable fast and reliable tool condition monitoring.

The computation of the DEFROL value is carried out according to the shape of drill tools; hence, it would be required to change this computation approach for different shaped tools, such as end mill or ball mill, which have not been investigated in this paper.

REFERENCES

1 **Thasty, J.** and **Smith, S.** Current trends in high-speed machining. *J. Mfg Sci. Engng, ASME*, 1997, (1119), 664–666.

2 **Kim, J.-H., Moon, D.-K., Lee, D.-W., Kim, J.-S., Kang, M.-C.,** and **Kim, K.-H.** Tool wear measuring technique on the machine using CCD and exclusive jig. *J. Mater. Proc. Technol.*, 2002, (131), 668–674.

3 **Konig, W., Langhammer, K.,** and **Schemmel, H. U.** Correlation between cutting force components and tool wear. *Ann. CIRP*, 1972, 19–20.

4 **Lindstrom, B.** and **Lindberg, B.** Measurement of dynamic cutting forces in the cutting process, a new sensor for in-process measurement. In Proceedings of the 24th International Machine Tool Design and Research Conference, 1983, pp. 137–147.

5 **Takeyama, H., Doi, Y., Mitsoka, T.** and **Sekiguchi, H.** Sensors of tool life for optimisation of machining. In Proceedings of the 8th International Machine Tool Design and Research Conference, 1967, pp. 191–208.

6 **Stoferle, T. H.** and **Bellmann, B.** Continuous measuring of flank wear. In Proceedings of the 16th International Machine Tool Design and Research Conference, 1975, pp. 573–578.

7 **Kurada, S.** and **Bradley, A.** A review of machine vision sensors for tool condition monitoring. *Computers in Ind.*, 1997, (34), 55–72.

8 **Tsai, D-M., Chen, J-J.,** and **Chen, J-F.** A vision system for surface roughness assessment using neural network. *Int. J. Advanced Mfg Technol.*, 1998, (14), 412–422.

9 **Mannan, M. A., Kassim, A. A.,** and **Jing, M.** Application of image and sound analysis techniques to monitor the condition of cutting tools. *Pattern Recognition Lett.*, 2000, (21), 969–979.

10 **Bradley, C.** and **Wong, Y. S.** Surface texture indicators of tool wear – a machine vision approach. *Int. J. Advanced Mfg Technol.*, 2001, (17), 435–443.

11 **Mannan, M. A.** and **Kassim, A. A.** Texture analysis using fractals for tool wear monitoring. In Proceedings of IEEE International Conference on *Image Processing*, 2002, 105–108.

12 **Sortino, M.** Application of statistical filtering for optical detection of tool wear. *Int. J. Mach. Tools Mfe*, 2003, (43), 493–497.

13 **Mannan, M. A., Mian, Z.** and **Kassim, A. A.** Tool wear monitoring using a fast Hough transform of images of machined surfaces. *Mach. Vision Applic.*, 2004, (15), 156–163.

14 **Jurkovic, J., Korosec, M.** and **Kopac, J.** New approach in tool wear measuring technique using CCD vision system. *Int. J. Mach. Tools Mfe.*, 2005, (45), 1023–1030.

15 **Yang, M-Y.,** and **Kwon, O-D.** A tool condition recognition system using image processing. *Control Engng Practice*, 1998, (6), 1389–1395.

16 **Lanzetta, M.** A new flexible high-resolution vision sensor for tool condition monitoring. *J. Mater. Processing Technol.*, 2002, (119), 73–82.

17 **Kerr, D., Pengilley, J.,** and **Garwood, R.** Assessment and visualization of machine tool wear using computer vision. *Int. J. Advanced Mfg Technol.* (published online) 2005.

18 **Wang, W., Wong, Y. S.,** and **Hong, G. S.** Flank wear measurement by successive image analysis. *Computers in Ind.*, 2005, (56), 816–830.

19 **Rehorn, A. G., Jiang, J.,** and **Orban, P. E.** State-of-the-art methods and results in tool condition monitoring: a review. *Int. J. Advanced Mfg Technol.*, 2005, (26), 693–710.

20 **Canny, J.** A computational approach to edge detection. *IEEE Trans. on Pattern Analysis and Mach. Intell.*, 1986, (8), 679–698.